British Journal of Pharmacology (2003) 138, 1259–1270
www.nature.com/bjp

Pharmacological discrimination between muscarinic receptor signal transduction cascades with bethanechol chloride

[1]Liwang Liu & *,[1]Ann R. Rittenhouse

[1]Program in Neuroscience, Program in Cellular & Molecular Physiology, Department of Physiology, University of Massachusetts Medical Center, 55 Lake Ave. North, Worcester, MA 01655, U.S.A.

1 Muscarinic agonist specificity is limited, making it difficult to match receptor subtypes with signal transduction cascades that mediate ion channel modulation. We have characterized the inhibitory effects of two muscarinic agonists, oxotremorine-M (Oxo-M) and bethanechol chloride (BeCh), on Ca^{2+} currents in neonatal rat superior cervical ganglion neurons.

2 Oxo-M-mediated (10 μM) inhibition occurred *via* two signaling pathways. The first pathway inhibited whole cell peak currents, consisting primarily of N-type current, but not FPL 64176-induced, long-lasting tail currents, comprised entirely of L-type current. Inhibited currents displayed slowed activation kinetics and voltage dependence, characteristics of membrane-delimited inhibition. Current inhibition was blocked by the selective M_2 receptor antagonist, methoctramine (METH; 100 nM), or following pertussis toxin (PTX) pretreatment.

3 Activation of the second pathway inhibited both peak and long-lasting tail currents. This pathway was voltage-independent, PTX-insensitive, but sensitive to internal Ca^{2+} chelator concentration. Muscarinic toxin 7 (MT-7, 100 nM), an irreversible M_1 receptor antagonist, eliminated this inhibition. Oxo-M (100 μM) decreased L- and N-type channel activities in cell-attached patches, indicating that a diffusible second messenger is involved.

4 BeCh (100 μM) also inhibited whole cell currents *via* the membrane-delimited pathway. Blocking M_4 receptors with 100 nM pirenzepine (in the presence of MT-7) had no effect, while antagonizing M_2 receptors with METH abolished inhibition. Concentrations of BeCh as high as 3 mM failed to inhibit either peak or long-lasting tail currents following PTX pretreatment.

5 These results indicate that BeCh may be an effective tool for selectively activating M_2 receptor stimulation of the membrane-delimited pathway.

British Journal of Pharmacology (2003) **138,** 1259–1270. doi:10.1038/sj.bjp.0705157

Keywords: Bethanechol; L-type calcium channels; N-type calcium channels; ω-Conotoxin GVIA; FPL 64176; (+)-202-791; G-proteins; M_1-muscarinic receptors; M_2-muscarinic receptors; nimodipine; oxotremorine-M

Abbreviations: BeCh, bethanechol chloride; ω-CgTx, ω-conotoxin GVIA; FPL, FPL 64176; METH, methoctramine; MT-7, muscarinic toxin 7; NMN, nimodipine; Oxo-M, oxotremorine-M; PTX, pertussis toxin; PRZ, pirenzepine; SCG, superior cervical ganglion; TTX, tetrodotoxin

Introduction

M_1–M_4 muscarinic receptors modulate the activity of a number of types of ion channels, apparently by multiple mechanisms, resulting in remarkably complex signaling (Hille, 1994). In adult superior cervical ganglion (SCG) neurons, muscarinic agonists activate multiple signaling pathways to inhibit Ca^{2+} currents (Hille, 1994; Shapiro *et al*., 2001). A fast (<1 s), pertussis toxin (PTX)-sensitive, membrane-delimited pathway, mediated by M_2/M_4 muscarinic receptors and G_o/G_i-like GTP-binding proteins, selectively inhibits whole cell N-type currents (Beech *et al*., 1991, 1992; Bernheim *et al*., 1992; Shapiro *et al*., 1999). Currents inhibited by this pathway exhibit slowed activation kinetics and a shift in the voltage sensitivity; a positive prepulse relieves inhibition (Ikeda, 1991; Beech *et al*., 1992).

A second pathway, mediated by M_1 muscarinic receptors and G_q-like G-proteins, appears to involve a diffusible second messenger because in cell-attached patches both L- and N-type Ca^{2+} channel activities decrease following application of the muscarinic agonist oxotremorine-M (Oxo-M) to the bath (Bernheim *et al*., 1991, 1992; Mathie *et al*., 1992; Shapiro *et al*., 1999; Haley *et al*., 2000). In contrast to the membrane-delimited pathway, the onset of this inhibition is slow ($\tau > 36$ s), PTX-insensitive, and requires a low concentration of internal divalent chelator, for example, 0.1 mM 1,2-bis (*o*-aminophenoxy) ethane-*N*,*N*,*N*′,*N*′-tetraacetic acid (BAPTA) at the whole cell level. This slower form of modulation is voltage-independent, suppressing whole cell Ca^{2+} currents equally at all test potentials (Bernheim *et al*., 1991; Beech *et al*., 1992).

Previously, the muscarinic agonist bethanechol chloride (BeCh) was used to examine the membrane-delimited pathway in neonatal SCG neurons (Plummer *et al*., 1991). Pretreatment with PTX completely blocked the inhibition of the current by BeCh, suggesting that only a PTX-sensitive, membrane-delimited pathway is present in neonatal cells. However, these studies were performed with an internal divalent cation

*Author for correspondence;
E-mail: Ann.Rittenhouse@umassmed.edu

chelator concentration of 10 mM EGTA, which may have minimized the muscarinic activation of the diffusible second messenger pathway. Currently, there is no way to examine independently the muscarinic modulation of these two pathways without changing conditions, for example, removing the membrane-delimited pathway with PTX or blocking the diffusible second messenger cascade by increasing the BAPTA concentration in the pipette, thereby generating data that are never completely comparable. Whether both pathways are present in neonatal SCG neurons thus remains unclear. Moreover, it is not known whether BeCh and Oxo-M share the same abilities to sufficiently stimulate both pathways, such that current modulation can be observed.

Therefore, in the present study, we examined whether muscarinic modulation of Ca^{2+} currents in neonatal rat SCG neurons displays the same characteristics as in adult neurons. We have found that in addition to the membrane-delimited pathway, a diffusible second messenger pathway is also present in the neonate. Moreover, in the process of clarifying muscarinic signaling in neonatal neurons, we have demonstrated the selective modulation of N-type current by M_2 receptor stimulation of the membrane-delimited pathway with BeCh. The identification of functional selectivity with BeCh is the first step towards independently manipulating these two muscarinic pathways under otherwise identical recording conditions.

Methods

Preparation of cells

SCG neurons of 1 to 3-day-old Sprague–Dawley rats (Charles River Laboratories, Wilmington, MA, U.S.A.) were isolated and mechanically dissociated (Hawrot & Patterson, 1979) following decapitation. The cells were plated on poly-L-lysine (Sigma, St Louis, MO, U.S.A.)-coated glass coverslips and cultured at 37°C, 5% CO_2 in Dulbecco's modified eagle's medium (DMEM; Sigma, St Louis, MO, U.S.A.), supplemented with 7.5% fetal calf serum (Sigma, St Louis, MO, U.S.A.), 7.5% fetal bovine serum (Sigma, St Louis, MO, U.S.A.), 4 mM glutamine, 100 U ml^{-1} penicillin, 100 μg ml^{-1} streptomycin (Sigma, St Louis, MO, U.S.A.), and 0.2 μg ml^{-1} nerve growth factor (Bioproducts for Science, Indianapolis, IN, U.S.A.). Cells were used within 12 h to avoid recording from cells with processes.

Current recordings

Whole cell and unitary Ca^{2+} currents were recorded with standard techniques (Hamill *et al.*, 1981). Pipette series resistance and capacitance were zeroed upon sealing. The currents were recorded at room temperature (20–24°C) with an Axopatch 200A patch-clamp amplifier (Axon Instruments, Foster City, CA, U.S.A.). For whole cell recordings, following breakthrough, capacitive transients were compensated by approximately 70%. Currents were low-pass filtered at 5 kHz using the four-pole Bessel filter in the clamp amplifier and sampled at 20 kHz except where noted. Cell-attached patch currents were filtered at 1 kHz and sampled at 5 kHz. All current traces were stored and later analyzed on the hard drive of a Pentium computer using CED Patch (version 6.3) acquisition and analysis programs (Cambridge Electronic Design Limited, Cambridge, U.K.). Electrodes were made from borosilicate glass capillaries (Drummond Scientific Company, Broomall, PA, U.S.A.) and fire-polished to a tip diameter of $\sim$1 μm. The total pipette access resistance ranged from 2.0 to 2.5 and 3.0 to 5.0 MΩ for whole cell and cell-attached patch electrodes, respectively. The external solution was grounded by an Ag–AgCl ground *via* a 140 mM KC1 agar bridge and bath.

In some recordings a voltage protocol, developed by Plummer *et al.* (1989) and modified by Liu *et al.* (2001), was used to isolate L-type currents. The membrane voltage was held at −90 mV, stepped to +10 mV for 20 ms and then stepped back to an intermediate potential of −40 mV. Under these conditions and in the presence of an L-type channel agonist in the bath, either FPL 64176 (FPL) or (+)-202-791, a long-lasting component of the tail current made up entirely of L-type current could be elicited (Liu *et al.*, 2001). Command pulses were delivered at 4-s intervals. Prior to analysis, leak and capacitive transients were eliminated from all records by scaling up the current recorded at −110 mV and then subtracting it from individual sweeps. In some figures, residual transients that remained after leak subtraction were removed. Peak current amplitudes were measured 10 ms after the start of the test pulse for experiments where the membrane-delimited pathway was specifically examined. For all other experiments, peak current amplitudes were measured 15 ms after the start of the test pulse. For experiments where the long-lasting component of the tail current was measured, a second cursor was placed approximately 13 ms following the test pulse. The long-lasting component of the control tail current (in the absence of the L-type channel agonist) typically measured approximately −5 pA in amplitude. Plots of long-lasting tail current *versus* test potential were obtained by stepping the test potential in 10 mV increments from −60 to +80 mV. Tail potential remained at −40 mV.

For cell-attached patch recordings of unitary L- and N-type channel activity, membrane patches were held at −90 mV and stepped to +30 mV for 700 ms every 4 s. All recordings were performed with the dihydropyridine L-type channel agonist (+)-202-791 (500 nM) present in the bath. Criteria for identifying unitary L- and N-type Ca^{2+} channel activity have been previously described in detail (Rittenhouse & Hess, 1994; Liu & Rittenhouse, 2000). Oxo-M (100 μM) was superfused slowly into the bath to avoid disrupting the high-resistance seal. Traces were leak subtracted by averaging null sweeps together and subtracting the average from each sweep. At least 80 sweeps were analyzed for control and Oxo-M conditions; the exact number of sweeps was matched for each recording.

Whole cell and cell-attached patch data are expressed as the mean current amplitude or the percent change in current ±standard error of the mean. Statistical significance was determined by either a Student's *t*-test for two means or a paired *t*-test. $P<0.05$ was considered significant.

Drugs and solutions

The external solution contained 20 mM barium acetate (BaAc), 125 mM *N*-methyl-D-glucamine (NMG)-aspartate, 10 mM 4-(2-hydroxyethyl)-l-piperazineethane-sulfonic acid (HEPES), and 0.001 mM tetrodotoxin (293 mOsM). Ba^{2+} was used as the charge carrier so that Ca^{2+}-dependent inactivation of L-type

currents was minimized (Imredy & Yue, 1994). In particular, BaAc was used to minimize whole cell Ba^{2+} current contamination with Cl^- currents. The pipette solution was composed of 123 mM cesium (Cs)-aspartate, 10 mM HEPES, 0.1 mM BAPTA, 5 mM $MgCl_2$, 4 mM ATP (Sigma, St Louis, MO, U.S.A.) and 0.4 mM GTP (Aldrich, Milwaukee, WI, U.S.A.) (264 mOsM). When 20 mM BAPTA was included in the pipette solution, the Cs-aspartate concentration was lowered accordingly in the pipette solution. For cell-attached patch recordings of unitary L- and N-type channel activity, the membrane potential was effectively zeroed with a bath solution containing 140 mM K^+ aspartate, 10 mM HEPES, 5 mM EGTA, and 0.5 μM (+)-202-791. The pipette solution contained 110 mM $BaCl_2$ and 10 mM HEPES. The pH of all solutions was adjusted to 7.5.

According to the requirements of each experiment, drugs were added to the external solution by superfusion. The L-type Ca^{2+} channel antagonist nimodipine and the agonists, FPL 64176 (RBI, Natick, MA, U.S.A. or Sigma) and (+)-202-791 (a gift from Dr Hof, Sandoz Corp., Switzerland), were prepared from stock solutions made up in 100% ethanol and diluted with the bath solution to a final ethanol concentration of less than 0.01%. The maximal final concentration of ethanol had no significant effect on currents. Stocks of ω-conotoxin GVIA (ω-CgTx) (Bachem, Torrance, CA, U.S.A.), muscarinic toxin 7 (MT-7, Peptides International, Inc., Osaka, Japan), BeCh, METH, Oxo-M, pirenzepine (PRZ), tetrodotoxin (TTX, RBI, Natick, MA, U.S.A. or Sigma) and PTX (List Biological Laboratories, Inc., Campbell, CA, U.S.A.) were made in double-distilled water. Stocks were subsequently diluted at least 1000-fold with external solution to their final concentration.

Results

Oxo-M inhibits both N- and L-type currents in neonatal SCG neurons

As a first step in determining whether the diffusible second messenger pathway is present in neonatal SCG neurons, we tested the ability of the muscarinic agonist Oxo-M to inhibit whole cell Ba^{2+} currents, when using a low divalent cation chelator concentration (0.1 mM BAPTA) in the pipette solution. Adding Oxo-M (10 μM) to the bath, in the continued presence of FPL 64176 (FPL), a nondihydropyridine L-type channel agonist (Rampe & Lacerda, 1991), inhibited the long-lasting tail current by 43$\pm$4% and the peak current by 51$\pm$8% (Figures 1a–c). The amount of inhibition of the peak current was greater than could be attributed to the L-type current, which normally makes up approximately 10% of the whole cell current in SCG neurons (Plummer *et al*., 1989). These results suggest that Oxo-M inhibits both L- and N-type currents. To verify that current inhibition was not simply because of Oxo-M interacting with FPL, the effects of Oxo-M were examined in the presence of the dihydropyridine L-type channel agonist (+)-202-791 (1 μM). No significant difference in the magnitude of inhibition of either the peak (44$\pm$4%) or the long-lasting tail (43$\pm$6%) current by 10 μM Oxo-M was found when (+)-202-791 *versus* FPL was used ($n=5$, data not shown). Moreover, because FPL and dihydropyridine agonists appear to bind to different sites on the channel (Rampe & Lacerda, 1991; but see Grabner *et al*., 1996), these results indicate that the inhibitory effects of Oxo-M are unlikely to be due to the displacement of L-type Ca^{2+} channel agonists.

We confirmed that L- and N-type currents were inhibited by Oxo-M by pharmacologically blocking L- or N-type current. First, SCG neurons were preincubated for at least 20 min in 5 mM Ca^{2+} tyrodes solution containing ω-CgTx (1 μM), which irreversibly blocks N-type current. No L-type channel agonist was present in the bath. When these cells were tested for their sensitivity to 3 μM Oxo-M, the current was decreased by 33$\pm$5% ($n=17$, data not shown), consistent with L-type current inhibition. In a second experiment, L-type channel activity was antagonized by including 1 μM nimodipine (NMN), an L-type Ca^{2+} channel antagonist, in the bath solution. In the continued presence of NMN, 3 μM Oxo-M inhibited the peak current by 49$\pm$8% ($n=4$; data not shown), demonstrating that N-type current also is inhibited. The ω-CgTx and NMN experiments were performed on PTX-treated cells. The finding that Oxo-M inhibits both the L- and the N-type current by a PTX-insensitive pathway suggests that the diffusible second messenger pathway, previously described in adult SCG neurons (Hille, 1994), may be present in neonatal neurons.

To confirm this, we examined whether application of Oxo-M to the bath could inhibit unitary L- and N-type channel activity in cell-attached patches. An example of the effect of Oxo-M on unitary L-type currents in a single channel patch is shown in Figure 2a and on N-type currents in a patch containing two N-type Ca^{2+} channels is shown in Figure 2b. When we examined the effect of Oxo-M on open probability (P_o), we found that P_o in two single L-type channel patches decreased by 51 and 80%. Oxo-M also decreased P_o in single N-type channel patches by 42$\pm$7% ($n=3$). Following bath application of 100 μM Oxo-M, mean ensemble currents in patches containing multiple channels significantly decreased ($P<0.05$) by 55$\pm$9% ($n=5$, data not shown). In contrast, in long recordings where no agonist was applied, activity in the first part of the recording showed no difference from activity in the second half of the recording (133$\pm$35% of initial activity; $P>0.05$; $n=3$, data not shown), indicating that channel activity during the recording time does not normally decrease. These recordings were of similar length to the Oxo-M-treated patches (no agonist, 76–190 sweeps/group *versus* Oxo-M-treated, 90–116 sweeps/group), indicating no time bias was present when comparing 'no agonist' and Oxo-M-treated patches. Taken together, these results indicate that in neonatal SCG neurons Oxo-M can inhibit both L- and N-type Ca^{2+} channel activity using a diffusible second messenger signaling pathway.

Oxo-M also stimulates the membrane-delimited pathway

At least one step in the diffusible second messenger pathway found in adult SCG neurons is sensitive to the BAPTA concentration in the pipette solution (Beech *et al*., 1991). If the same diffusible second messenger pathway is present in neonatal SCG neurons, raising the BAPTA concentration from 0.1 to 20 mM should block it, but leave the membrane-delimited pathway intact. Thus, if the membrane-delimited pathway is activated by Oxo-M under 'high BAPTA' conditions, we would expect to observe inhibition of the peak current, but a loss of inhibition of the long-lasting tail current.

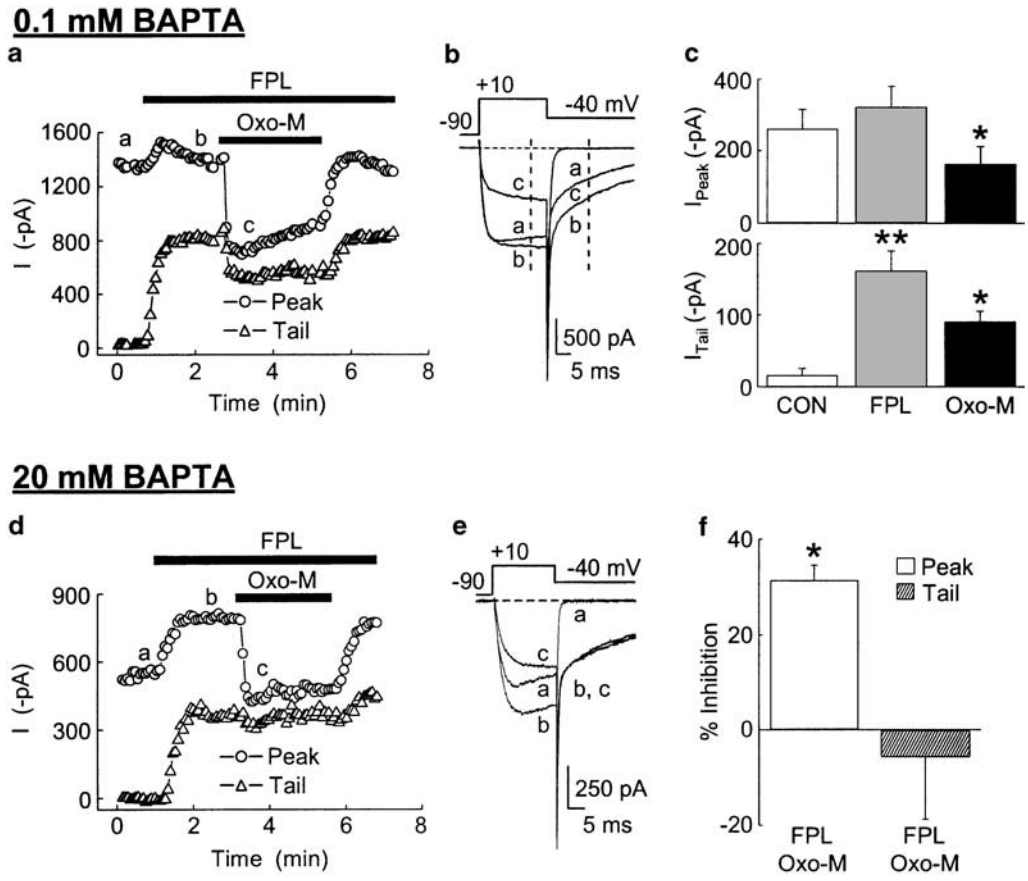

Figure 1 The muscarinic agonist Oxo-M (10 μM) rapidly and reversibly inhibits both peak and long-lasting tail currents in rat neonatal SCG neurons. This inhibition can be observed in the example of peak (upper plot) and tail (lower plot) current amplitudes *versus* time (a) and in the individual sweeps (b) taken from the time course, where indicated. A nondihydropyridine L-type Ca^{2+} channel agonist, FPL 64176 (FPL; 1 μM), included in the bath solution, elicited a large, long-lasting component of the tail current (a–c). In contrast, FPL induced only a modest increase of $20\pm5\%$ in the peak current. The amplitudes of the peak and the long-lasting component of the tail current were measured in individual sweeps shown in (b) by the vertical left and right dotted lines respectively. This protocol was used in all the following experiments unless otherwise stated. The effects of Oxo-M and FPL on mean peak and long-lasting tail currents are summarized in (c). Oxo-M inhibited peak currents by $51\pm8\%$ and tail currents by $43\pm4\%$. $^*P<0.05$, compared to FPL levels using a two-tailed, paired *t*-test ($n=4$); $^{**}P<0.01$, compared to CON levels using a two-tailed, paired *t*-test ($n=4$). (d–f) Inhibition of the long-lasting tail current was lost when 20 mM BAPTA was included in the pipette solution. (d) Example time course of the rapid and reversible inhibition of the peak current (upper plot) with no inhibition of the long-lasting tail current (lower plot). (e) Selected sweeps taken from (d) at the times indicated. (f) Oxo-M significantly decreased the peak current (open bar) by $32\pm3\%$ in the continued presence of FPL ($^*P<0.05$; $n=6$), but had no significant effect on the long-lasting tail current ($-6\pm13\%$ of FPL levels; $P>0.05$; $n=6$).

Under these conditions, rapid, reversible inhibition of the peak current by Oxo-M remained; however, Oxo-M-induced inhibition of the long-lasting tail current was lost (Figures 1d–f). Furthermore, inhibited currents exhibited slowed activation kinetics (Figure 1e) characteristic of the membrane-delimited inhibition of N-type current (Wanke *et al*., 1987; Bean, 1989; Plummer *et al*., 1991; Beech *et al*., 1992). Following application of Oxo-M, the time to peak current increased significantly from 13.9 ± 1.3 to 17.8 ± 0.5 ms ($P<0.05$; $n=6$, data not shown). These results indicate that raising the BAPTA concentration blocks the diffusible second messenger pathway, revealing the membrane-delimited pathway.

The above findings indicate that both the diffusible second messenger and the membrane-delimited pathways are present in the neonate. Current modulation by these two pathways can be demonstrated further by examining the voltage dependency of inhibition. Inhibition of N-type current in adult SCG neurons by the membrane-delimited pathway has a component that is voltage-dependent; a strongly positive prepulse can relieve this form of inhibition (Elmslie *et al*., 1990; Ikeda, 1991). Therefore, we tested whether a component of inhibition could be relieved with a prepulse. Voltage protocols were alternated every 4 s where cells were exposed to either a 200 ms prepulse to +80 mV, or no prepulse, followed 5 ms later by a test pulse to +10 mV (Figure 3a, inset).

Since current inhibition by the diffusible second messenger pathway is independent of voltage, the component of the inhibition by this pathway should remain following a prepulse under conditions of low divalent chelator (0.1 mM BAPTA in the pipette solution). Previously, we found that following a prepulse, the magnitude of current inhibition by Oxo-M was reduced by approximately 50%; however, significant inhibition remained (Liu & Rittenhouse, 2003). These results indicate that both a voltage-dependent and - independent component of inhibition are stimulated with Oxo-M under

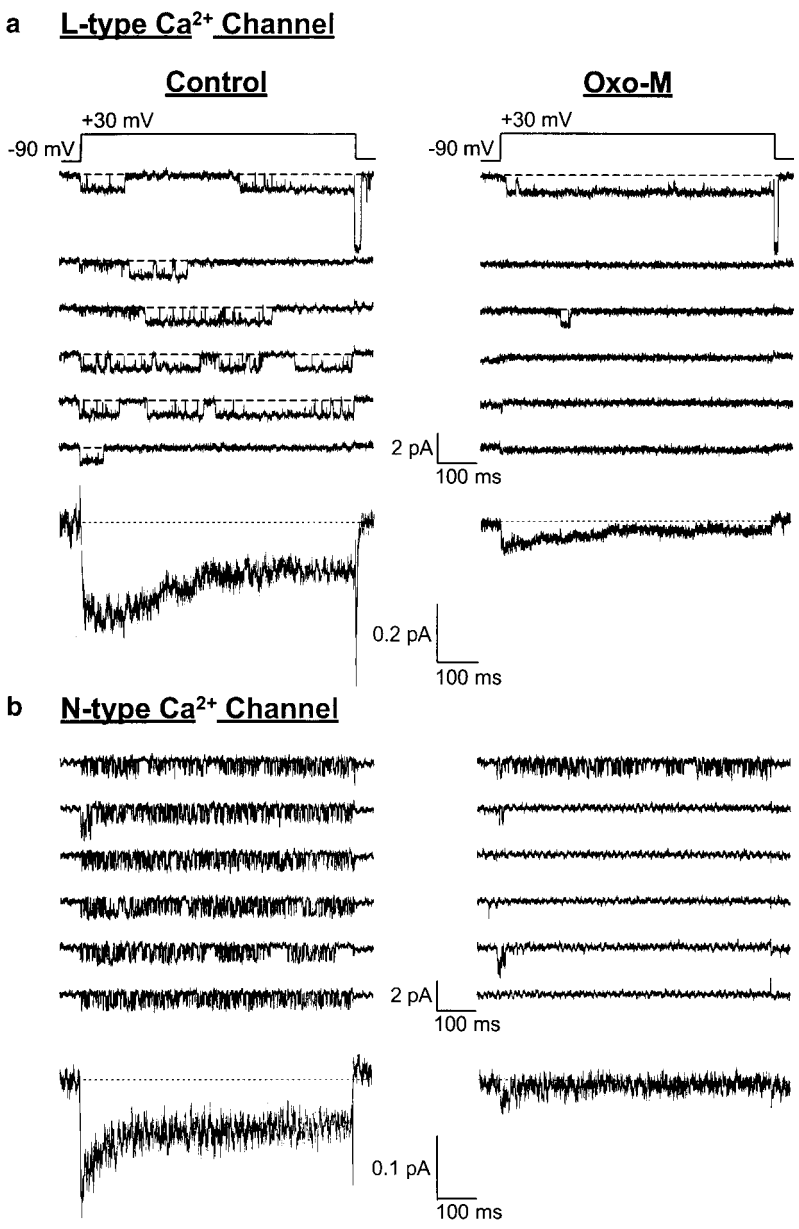

Figure 2 Application of Oxo-M to the bath inhibits unitary L- and N-type channel activity in cell-attached patches. (a, b) Left panel: Six consecutive control sweeps with mean ensemble trace below. Right panel: Six consecutive sweeps following treatment with 100 μM Oxo-M with mean ensemble trace below. (a) A patch with a single L-type channel. Consecutive sweeps were selected by starting with a trace that displayed a characteristic dihydropyridine-induced tail current. Mean ensemble traces were each constructed from 102 sweeps. (b) A patch with two N-type channels. Mean ensemble traces were each constructed from 87 sweeps.

conditions of low divalent chelator. When a higher concentration of chelator (10 mM EGTA) was used in the pipette solution, Oxo-M decreased the current by $55\pm6\%$ ($n=9$) from control levels (Figure 3a, left traces; Figure 3b, left bars). However, the majority of the Oxo-M-induced inhibition could now be relieved with a prepulse (Figure 3a, right traces; Figure 3b, right bars). No significant voltage-independent inhibition remained; current inhibition was reduced to a $16\pm8\%$ decrease ($P>0.05$, $n=9$). These latter findings indicate that in neonatal SCG neurons, all of the membrane-delimited inhibition induced by Oxo-M can be relieved with a prepulse. These results are consistent with current–voltage results, where the magnitude of inhibition decreased with increasing test potential (data not shown). In contrast, the magnitude of the inhibition of the long-lasting tail current (Figures 4a and c) showed no significant voltage dependence, consistent with inhibition of L-type current by the diffusible second messenger pathway.

Discrimination between two muscarinic signaling pathways with BeCh

BeCh inhibits the N-type current in neonatal SCG neurons by a PTX-sensitive, membrane-delimited pathway (Plummer *et al.*, 1991) when 10 mM EGTA was included in the pipette as the divalent cation chelator. Under these conditions, there was no obvious inhibition of the long-lasting tail current; however, the EGTA may have blocked L-type current inhibition by the

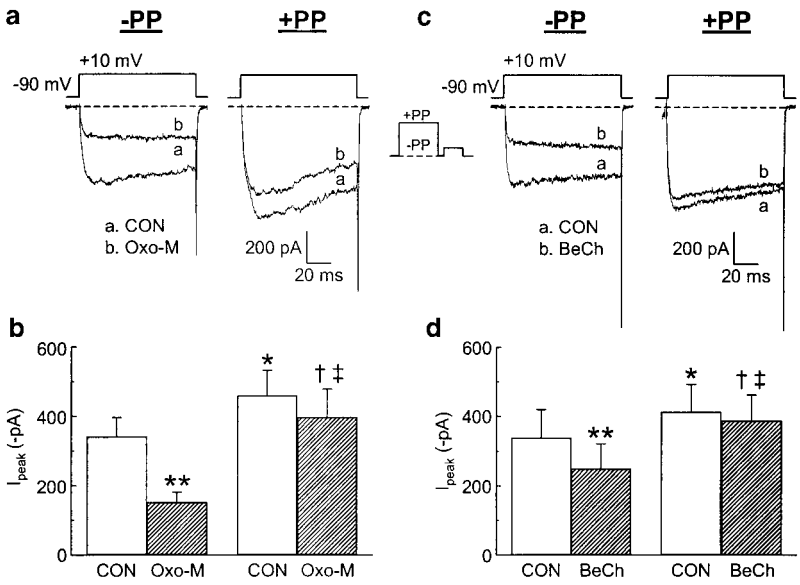

Figure 3 Both Oxo-M and BeCh elicit voltage-dependent inhibition of peak currents. (a) Inset: test currents were generated using a double pulse protocol that alternated every 4 s between a 200 ms prepulse to +80 mV (+PP) or no prepulse (−PP). After a brief (5 ms) return to −90 mV, the cell was stepped to +10 mV for 100 ms. The majority of current inhibition by 10 μM Oxo-M in high chelator concentration (10 mM EGTA) could be relieved with a prepulse. (a) Left sweeps and (b) left bars: Oxo-M decreased −PP currents compared to paired −PP controls (CON, $^{**}P<0.01$) by 54.5±5.7%. (a) Right sweeps and (b) right bars: Following a prepulse (+PP), significant facilitation of CON ($^{*}P<0.05$, compared to −PP CON) and Oxo-M currents ($^{\dagger}P<0.01$, compared to −PP Oxo-M) occurred. (c, d) Under low BAPTA (0.1 mM) conditions, current facilitation of 30±10% ($^{*}P<0.05$, −PP CON compared to +PP CON) occurred. (c) Left sweeps and (d) Left bars: 100 μM BeCh decreased −PP current by 31±7% ($^{**}P<0.01$ compared to −PP CON). (c) Right traces; (d) Right bars: Following a prepulse, inhibition by BeCh was relieved ($^{\dagger}P<0.01$, compared to −PP BeCh); no significant inhibition ($^{\ddagger}P>0.05$, compared to +PP CON) remained (5±4%). Each statistical analysis used a two-tailed paired *t*-test ($n=8-9$ recordings/group).

diffusible second messenger pathway. More recently, BeCh has been described as a muscarinic receptor agonist with low potency for binding to recombinant M_1 muscarinic receptors (Richards & van Giersbergen, 1995). However, BeCh can stimulate both PI hydrolysis 12-fold and arachidonic acid release at least 15-fold in recombinant systems, both measures of M_1 receptor-activated signal transduction cascades (Wang & El-Fakahany, 1993; Richards & van Giersbergen, 1995; Bymaster *et al*., 1999). These findings suggest that, despite its low potency for binding, BeCh can confer M_1 receptor activity. Thus, whether submillimolar concentrations of BeCh can activate the diffusible second messenger pathway sufficiently to cause functional changes in Ca^{2+} channel activity was unclear. To test whether BeCh can inhibit L- and N-type currents by the diffusible second messenger pathway, currents were recorded in the presence of FPL (in the bath) and 0.1 mM BAPTA (in the pipette solution), conditions that optimize the activity of this pathway. Under these conditions, BeCh (100 μM) had no obvious effect on the long-lasting tail current, but rapidly inhibited the peak current by 38.2±5.7% (Figures 4b and c and 5a, b and e). The inhibited current displayed slowed activation kinetics; BeCh significantly increased the time to peak current from 15.9±0.5 to 17.9±0.3 ($P<0.01$; $n=11$, data not shown). These data suggest that BeCh stimulates the membrane-delimited pathway, but not the diffusible second messenger pathway.

It is possible that BeCh can inhibit N-type current by the diffusible second messenger pathway, but the membrane-delimited pathway obscures the inhibition. If BeCh selectively stimulates the membrane-delimited pathway, all of the inhibition should be relieved with a prepulse; no voltage-independent inhibition should be observed. To determine whether BeCh stimulates voltage-independent inhibition, the prepulse protocol was employed. With low BAPTA (0.1 mM) in the pipette solution, a significant amount of facilitation of control currents occurred following a prepulse (30±10%), indicating the presence of tonic G-protein activity (Figure 3). Relief of tonic and BeCh-induced inhibition can be observed in selected sweeps shown in Figure 3c. Upon application of BeCh, unfacilitated (−PP) current amplitude decreased by 31±7% (Figure 3d, left bars). Following a prepulse (+PP), inhibition decreased to 5±4% and was no longer significant (Figure 3d, right bars), indicating that no inhibition by a voltage-independent pathway occurred. Moreover, plots of the long-lasting tail current, measured at −40 mV, *versus* test potential confirm that L-type current was unaffected by BeCh at any voltage (Figures 4b and c). Taken together, these results demonstrate that 100 μM BeCh causes no stimulation of the diffusible second messenger pathway. Furthermore, with low divalent cation chelator (0.1 mM BAPTA), BeCh's effects on the membrane-delimited pathway remain similar to those observed previously where 10 mM EGTA was used as chelator (Plummer *et al*., 1991).

If the actions of 100 μM BeCh are selective for the membrane-delimited pathway, while Oxo-M is able to stimulate both pathways, then removing the membrane-delimited pathway should result in the loss of current inhibition by BeCh, but inhibition of the peak and the long-lasting tail currents by Oxo-M should remain. The membrane-delimited pathway can be rendered inoperative by preincubating neurons with 500 ng ml^{-1} of PTX for at least 5 h prior to recording their currents. An example plot of current

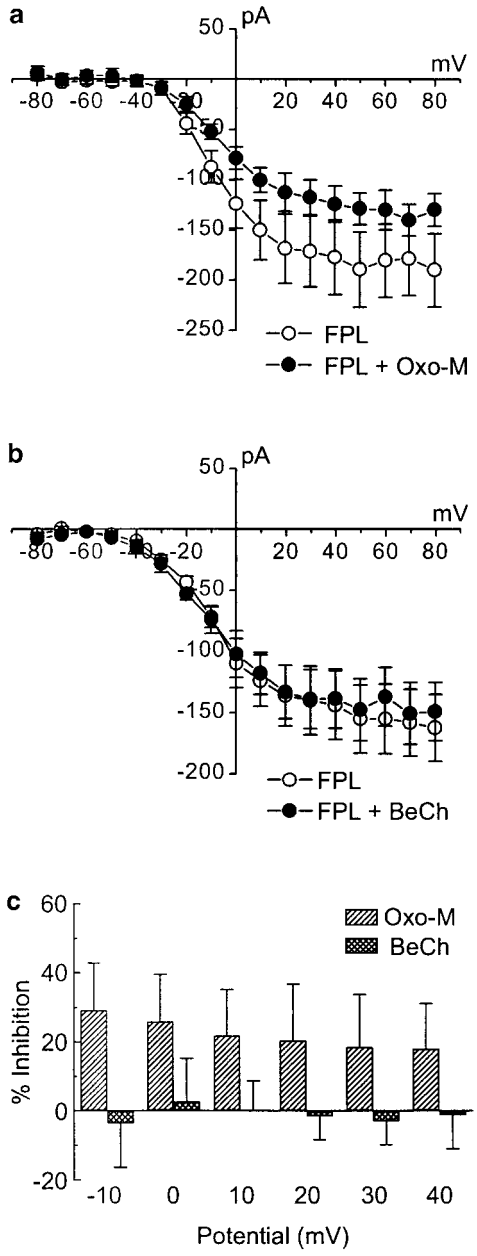

Figure 4 Oxo-M, but not BeCh, inhibits long-lasting tail currents independently of test potential. The plots of tail current *versus* test potential show that while Oxo-M (10 μM) inhibited at all potentials approximately 22% (a), BeCh (100 μM) had no effect on the long-lasting tail current at any potential (b); $n=4-6$ recordings/data point. (c) Plot of the percent inhibition of the long-lasting tail currents *versus* test potential taken from (a) and (b). Analysis of variance indicates that the percent inhibition of the long-lasting tail current did not vary significantly with voltage ($P>0.05$), demonstrating that this form of inhibition is voltage-independent.

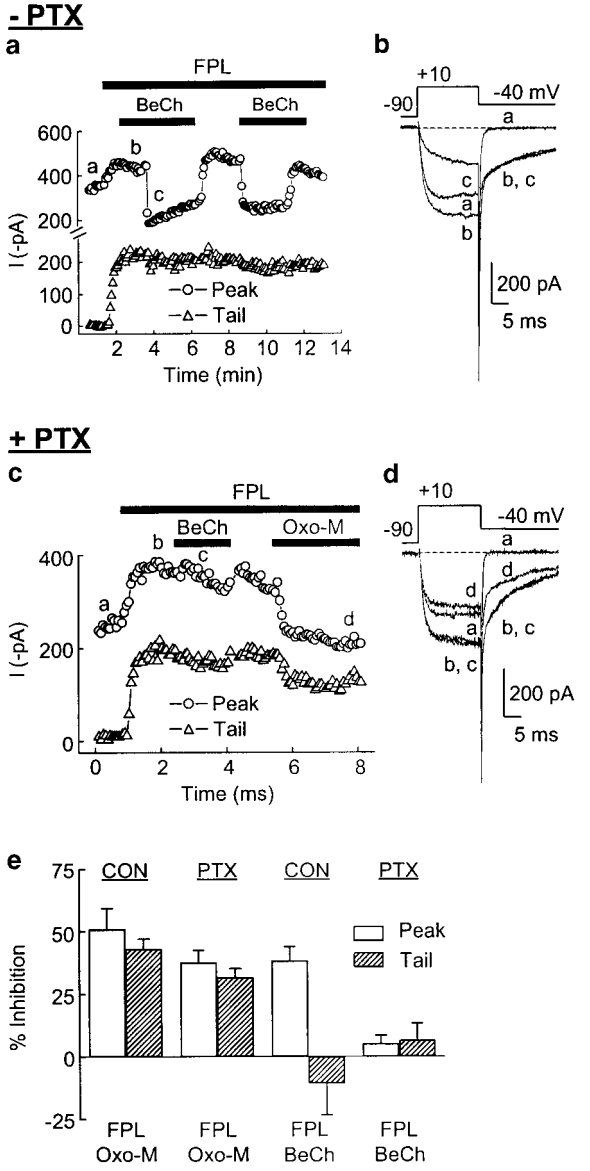

Figure 5 BeCh selectively inhibits N-type current by a PTX sensitive pathway. A low BAPTA concentration (0.1 mM) was used in the pipette solution. In plots of peak (upper plot) and tail (lower plot) current *versus* time (a) and in individual sweeps (b), BeCh (100 μM) rapidly and reversibly inhibited the peak current, but had no effect on the long-lasting tail current. (c) In PTX pretreated cells, BeCh (100 μM) lost its ability to inhibit the peak current, while 10 μM Oxo-M still inhibited both the peak and the long-lasting tail current. (d) Individual traces taken from (c) were noted. (e) Oxo-M inhibited peak current by $51\pm4\%$ ($n=4$), while BeCh inhibited the current by $38.2\pm5.7\%$ ($n=3$). Following PTX treatment, Oxo-M still inhibited both the peak by $31\pm6\%$ and the long-lasting tail current by 26 ± 4 %, while BeCh inhibition of peak current was largely eliminated; inhibition was not significant ($5\pm7\%$, $n=4$ cell recordings/group). The magnitude of tail current inhibition by Oxo-M in the presence of PTX was not significantly different than under normal conditions.

versus time is shown in Figure 5c with corresponding selected sweeps (Figure 5d). Following PTX pretreatment, the inhibition of the peak current by BeCh was largely eliminated, while Oxo-M still inhibited both the peak and the long-lasting tail currents. The actions of BeCh and Oxo-M on whole cell currents are summarized in Figure 5e. Oxo-M was able to inhibit significantly both the peak and the long-lasting tail current in untreated and PTX-treated cells, demonstrating that the diffusible second messenger pathway is PTX-insensitive in neonatal neurons and active under these experimental conditions. BeCh shows a different profile of current modulation. With PTX-treatment, no significant inhibition of either the peak or the long-lasting tail current could be detected (Figures 5c–e), suggesting that BeCh is unable to convey modulation of

L- and N-type currents by the diffusible second messenger pathway.

Although BeCh was used at a 10-fold higher concentration than Oxo-M, it is possible that BeCh can indeed stimulate the diffusible second messenger pathway, but requires a concentration greater than 100 μM. To examine this possibility, BeCh was tested from 0.01 to 3000 μM for its ability to inhibit peak current of untreated and PTX-treated cells. Concentrations of Oxo-M, ranging from 0.01 to 100 μM, were also tested for comparison. Both BeCh and Oxo-M showed a concentration-dependent inhibition of peak currents in untreated cells (Figures 6a and b). Maximal inhibition was 44 ± 3 and $57\pm4\%$ for 30 μM BeCh and 30 μM Oxo-M, respectively. Higher concentrations of either agonist were unable to increase inhibition significantly, most likely reflecting the underlying mechanisms involved. First, as shown above in the prepulse studies, under control conditions, a component of current is inhibited by tonically active G-proteins, resulting in an under representation of the total maximal inhibition that could occur with agonist. Second, membrane-delimited inhibition is voltage-dependent (Bean, 1989; Elmslie *et al.*, 1990; Ikeda, 1991) and is relieved with positive test pulses, giving rise to currents with slowed activation kinetics. Lastly, inhibition *via* the diffusible second messenger pathway results in an increase in null sweeps (Mathie *et al.*, 1992) raising the possibility that inhibited channels are stabilized in an inactivated state. Depending on the transition rates out of inactivated states, this form of inhibition also may not be absorbing. At any given instant, only a certain percentage of channels will be available to open, and thus, the predicted maximal inhibition will always be less than 100%.

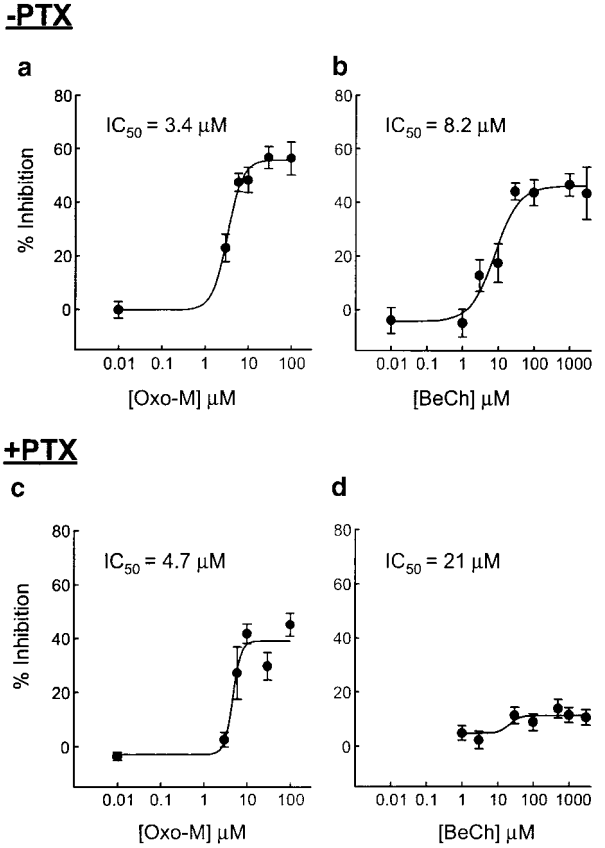

Figure 6 Inhibition of peak current by BeCh was largely lost following PTX pretreatment. Inhibition of peak currents under control (−PTX) conditions (a, b) and pretreatment with PTX (+PTX) (c, d) were measured for varying concentrations of Oxo-M and BeCh. A low BAPTA concentration (0.1 mM) was used in the pipette solution. Current amplitude was measured either after 2 min of superfusion with the muscarinic agonist or upon reaching a steady-state level. Current amplitudes were measured at a test potential of +10 mV (3–9 recordings/data point). Data were best fitted with the use of sigmoidal nonlinear regression curves.

When cells were pretreated with PTX to block the membrane-delimited pathway, the inhibition of peak current by BeCh was largely lost; maximal inhibition of $11\pm3\%$ occurred at 30 μM. Higher concentrations did not significantly increase inhibition (Figure 6d). In contrast, Oxo-M inhibited the peak current in PTX-treated cells in a concentration-dependent manner similar to untreated conditions; maximal inhibition of $45\pm4\%$ occurred at 10 μM (Figure 6c). These data indicate that whereas Oxo-M stimulates the PTX-sensitive, membrane-delimited pathway and the diffusible second messenger pathway, BeCh appears to act as a selective agonist of the PTX-sensitive, membrane-delimited pathway.

We next determined which muscarinic receptor mediated current inhibition by BeCh. Previous pharmacological studies indicated that inhibition of currents by the membrane-delimited pathway involved an M_2 receptor in adult mouse SCG (Shapiro *et al.*, 1999) but an M_4 receptor in older (~2–6 week) rat SCG neurons (Bernheim *et al.*, 1992; Fernandez-Fernandez *et al.*, 1999). To isolate M_2 and M_4 from M_1 receptors, cells were preincubated for at least 1 h (37°C) with 100 nM MT-7, which irreversibly binds to and blocks the function of M_1 receptors (Adem & Karlsson, 1997). Following this pretreatment, current inhibition by BeCh (100 μM) was $41\pm6\%$ (Figure 7). The magnitude of current inhibition was not significantly different ($P>0.05$ using a two way, *t*-test for two means, $n=3$–6 per group) from inhibition in the absence of MT-7 (Figure 5e), confirming that BeCh exerts its effects independently of M_1 receptors.

To determine whether M_4 receptors mediated current inhibition by the membrane-delimited pathway, 100 nM PRZ, a selective antagonist for M_4 receptors when cells already have their M_1 receptors blocked with MT-7, was included in the bath solution (Buckley *et al.*, 1989). Again, the magnitude of inhibition ($37\pm7\%$, $n=7$) was not significantly different from inhibition in the absence of antagonists ($P>0.05$ using a two-*t*-test for two means; $n=6$–7 per group), suggesting that another muscarinic receptor may mediate BeCh's effect. Therefore, we tested whether M_2 receptors mediated BeCh's actions by preincubating cells in MT-7 and including the selective M_2 receptor antagonist METH (100 nM) in the bath along with PRZ (Buckley *et al.*, 1989). Under these conditions, inhibition by BeCh was abolished ($-4\pm3\%$, $n=6$), suggesting that M_2 receptors mediate BeCh's actions (Figure 7). However, it was also possible that both M_2 and M_4 receptors had to be blocked in order to lose current inhibition. To test whether antagonizing M_2 but not M_4 receptors was sufficient to block BeCh's actions, only METH was included in the bath solution. Under these conditions, inhibition by BeCh was again eliminated ($-15\pm3\%$, $n=6$); the small increase in current was not significant ($P>0.05$). These findings indicate that BeCh inhibits currents by selectively activating M_2 receptors.

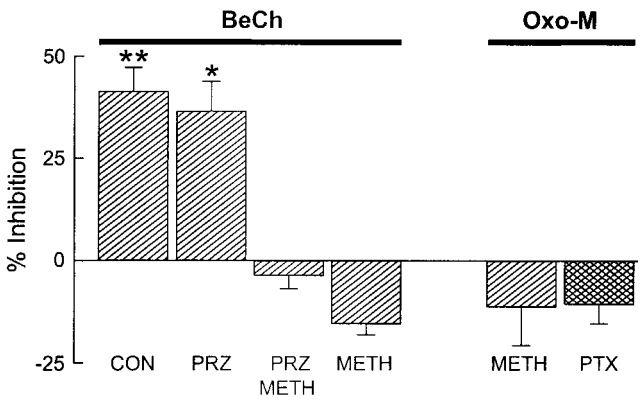

Figure 7 M_1 and M_2 muscarinic receptors mediate current inhibition by BeCh and Oxo-M. Cells were preincubated at 37°C in DMEM containing the irreversible M_1-selective antagonist MT-7 (100 nM) for at least 1 h. Hatched bars: Whole cell currents were then tested for their sensitivity to 100 μM BeCh or 10 μM Oxo-M when M_4 receptors and/or M_2 receptors were antagonized with 100 nM PRZ and/or 100 nM METH, respectively, by including them in the bath solution. BeCh inhibited currents when no additional antagonists were added to the bath by 41± 6% (**$P<0.01$); in the presence of PRZ by 37±7% (*$P<0.05$); in the presence of PRZ and METH by −4±3% ($P>0.05$); in the presence of METH, by −15±3% ($P>0.05$). Oxo-M inhibited currents in the presence of METH by −11±9% ($P>0.05$). Crosshatched bar: Following pretreatment with 500 ng ml^{-1} PTX for 5 h, Oxo-M inhibited currents by −11±5% ($P>0.05$). $n=6-7$ recordings/group.

These results are complementary to binding data (Richards & van Giersbergen, 1995) but somewhat surprising since previous studies indicated that M_4 receptors mediated Oxo-M-induced current inhibition by the membrane-delimited pathway in adult rat SCG neurons (Bernheim *et al*., 1992). Therefore, we tested whether M_2 receptors also mediated Oxo-M's effects on the membrane-delimited pathway in the neonate. When cells were pretreated with MT-7 to block M_1 receptors and METH (100 nM) was included in the bath, current inhibition by Oxo-M was eliminated (−11±9%, $n=6$); no significant change in the current occurred ($P>0.05$). These data indicate that Oxo-M also appears to primarily use the M_2 receptor to mediate the membrane-delimited pathway. However, in four of the cells, current inhibition was not only blocked, current actually increased with Oxo-M. On the contrary, in the two other cells, the current was inhibited by 9% and 24%, raising the possibility that a small amount of M_4 receptor stimulation also participates in current inhibition.

Finally, previous findings indicated that in adult SCG neurons, Oxo-M inhibits currents *via* the diffusible second messenger pathway using a M_1 receptor (Bernheim *et al*., 1992; Shapiro *et al*., 1999). To determine whether M_1 receptors mediated the diffusible second messenger pathway in neonatal SCG neurons, cells were preincubated for at least 5 h with PTX to disable the membrane-delimited pathway and pretreated for at least 1 h with MT-7 to irreversibly block M_1 receptors. With these conditions, current inhibition by Oxo-M (10 μM) was abolished (−11±5%, $n=7$); no significant change in the current occurred ($P>0.05$), indicating that M_1 receptors are required for activation of the diffusible second messenger pathway in neonatal SCG neurons.

Discussion

Muscarinic-induced inhibition of Ca^{2+} currents in neonatal SCG neurons occurs by both a PTX-sensitive, membrane-delimited and a diffusible second messenger pathway

Muscarinic-mediated inhibition of voltage-gated Ca^{2+} currents in acutely dissociated neonatal rat SCG neurons exhibits characteristics similar, although not identical to those observed in adult SCG neurons (Shapiro *et al*., 2001). We found that the muscarinic agonist Oxo-M inhibits both the peak current, comprised primarily of N-type current, and the long-lasting component of the tail current, elicited by FPL or (+)-202-791, and comprised solely of L-type current. Activation of two signal transduction pathways appears to account for the inhibition. A PTX-sensitive, voltage-dependent, membrane-delimited pathway, described previously for neonatal SCG neurons (Wanke *et al*., 1987; Plummer *et al*., 1991), selectively inhibits the peak current and slows the activation kinetics. A second pathway inhibits both the peak and the long-lasting tail currents. This form of inhibition has the characteristics reported previously for the diffusible second messenger pathway in adult SCG neurons: voltage-independence, PTX-insensitivity, BAPTA-sensitivity, and involvement of a signaling molecule that can cross the high-resistance seal to inhibit both L- and N-type channel activity in cell-attached patches (Beech *et al*., 1991, 1992; Bernheim *et al*., 1991; Mathie *et al*., 1992). Furthermore, we found that the acetylcholine derivative BeCh (Taylor, 1980) exhibits selective activation of the membrane-delimited pathway.

Our results resolve uncertainties in the literature surrounding muscarinic receptor-mediated modulation of Ca^{2+} currents in SCG neurons. Using BeCh, Plummer *et al*. (1991) found evidence of muscarinic stimulation of the membrane-delimited pathway. In contrast, Oxo-M activated both a fast, membrane-delimited pathway and a slower, diffusible second messenger pathway (Hille, 1994). Current inhibition *via* this latter pathway was observed only when the BAPTA concentration in the pipette solution was lowered to submillimolar concentrations. Sensitivity to the BAPTA concentration appears to be due in part to a Ca^{2+}-sensitive component in the signaling cascade, since raising the internal Ca^{2+} concentration restored part of the muscarinic inhibition of whole cell Ca^{2-} currents (Beech *et al*., 1991). A component of the inhibition could not be restored, however, suggesting that BAPTA itself in some way compromises this pathway.

The conditions used by Plummer *et al*. (1991) differed from those of the Hille lab in three potentially important ways. First, neonatal rather than adult SCG neurons were used. In these cells, Ca^{2+} channel inhibition appears simpler since the membrane-delimited pathway is entirely blocked by PTX, whereas in adult cells a component of inhibition is insensitive to PTX (Plummer *et al*., 1991; Beech *et al*., 1992). Second, BeCh rather than Oxo-M was used as the muscarinic agonist. Whether they share similar abilities to stimulate both muscarinic signal transduction cascades to modulate Ca^{2+} currents has not been documented previously. Third, 10 mM EGTA *versus* 0.1 mM BAPTA was used as the internal divalent cation chelator. While high concentrations of BAPTA (20 mM) block the diffusible second messenger cascade (Beech *et al*., 1991), it was unclear whether 10 mM EGTA can effectively

chelate divalent cations low enough to minimize the diffusible second messenger pathway.

To resolve these differences, we tested whether the diffusible second messenger pathway was present in neonatal cells using conditions previously employed for the adult (Beech *et al*., 1991). We found that when the divalent cation chelator concentration is changed to 0.1 mM BAPTA, Oxo-M can indeed inhibit both the peak and the long-lasting tail current demonstrating that this form of modulation also is expressed by parturition. Knockout studies in mouse models have confirmed previous pharmacological studies that M_1 muscarinic receptors couple to a diffusible second messenger pathway to inhibit both L- and N-type Ca^{2+} channel activities (Bernheim *et al*., 1991, 1992; Beech *et al*., 1992; Shapiro *et al*., 1999). Our data indicate that as in the adult, M_1 receptors mediate the Oxo-M-induced diffusible second messenger effect in the neonate. However, our prepulse experiments show that this second pathway would not have been detected previously in neonatal SCG neurons because the presence of 10 mM EGTA in the pipette solution is sufficient to block this form of inhibition (Figure 3; Liu & Rittenhouse, 2003).

Bethanechol selectively activates the membrane-delimited pathway

Furthermore, our results show that under conditions using 0.1 BAPTA, BeCh has a low potency for stimulating the diffusible second messenger pathway in neonatal SCG neurons. Following PTX pretreatment to eliminate the membrane-delimited pathway, the concentration–response curve for BeCh showed a maximum inhibition of only 11% even with concentrations as high as 3 mM. This result contrasts with the BeCh-induced inhibition of 44% in untreated cells. Moreover, when M_1 receptors were blocked with MT-7, BeCh-induced inhibition remained unaffected, indicating that while BeCh is unable to stimulate the diffusible second messenger pathway, it causes robust activation of the membrane-delimited pathway (Figures 3–7).

The BeCh results were somewhat unexpected, since, in general, binding studies show that agonists have poor selectivity for muscarinic receptor subtypes and few have been tested for functional selectivity (see Caulfield & Birdsall, 1998). However, under controlled conditions where recombinant muscarinic receptors were each expressed singly in CHO cells, BeCh exhibits selective binding with an order of potency of $M_2 > M_4 > M_3 > M_1$. Indeed, more than a 70-fold difference in IC_{50}s exists for BeCh-induced displacement of [^{3}H]-*N*-methylscopolamine binding between M_1 and M_2 receptors (Richards & van Giersbergen, 1995). Despite this low potency for binding to M_1 receptors, millimolar concentrations of BeCh stimulate PI hydrolysis 12-fold (Wang & El-Fakahany, 1993) and micromolar concentrations increase free arachidonic acid at least 15-fold ($EC_{50} = 7.7\,\mu$M) in recombinant systems (Bymaster *et al*., 1999). These values are both approximately two-thirds the values obtained with Oxo-M (Wang & El-Fakahany, 1993; Bymaster *et al*., 1999), suggesting that the activity conferred by BeCh binding to M_1 receptors should be sufficient to exert functional consequences in neurons such as modulation of Ca^{2+} channel activity. If BeCh does bind to M_1 receptors in neonatal SCG neurons, insufficient stimulation of the diffusible second messenger pathway occurs to cause functional changes in whole cell Ca^{2+} currents.

M_2 receptors mediate the fast, PTX-sensitive, membrane-delimited pathway in neonatal SCG neurons

Cloned muscarinic receptors have not always exhibited pharmacological profiles identical to *in vivo* receptors, possibly because of differences in post-translational modifications that then differentially affect binding and/or signal transduction (see Caulfield, 1993). However, in the case of BeCh and Oxo-M, our findings in neonatal SCG neurons do complement these previous binding studies (Richards & van Giersbergen, 1995). Whereas BeCh is a poor agonist for M_1 signaling, it selectively activates the membrane-delimited pathway by M_2 receptors; blocking M_4 receptors with 100 nM PRZ (in the presence of MT-7) had no effect on the ability of 100 μM BeCh to inhibit currents. In contrast, blocking M_2 receptors with 100 nM METH abolished current inhibition. Moreover, our results indicate that Oxo-M's effects on the membrane-delimited pathway also are primarily mediated by the M_2 receptor since METH also eliminated current inhibition by 10 μM Oxo-M. Interestingly, when we used pharmacological conditions that minimized the membrane-delimited pathway (Figure 7), we consistently observed a small, though statistically insignificant, enhancement of current. This may be because of decreased basal activity of PTX-sensitive G-proteins, resulting in relief of tonic inhibition. Another possibility is that an additional form of muscarinic modulation is revealed when this pathway is blocked.

Our results are consistent with patch-clamp studies examining Oxo-M-induced inhibition of Ca^{2+} currents in 11 to 14-day-old rat magnocellular basal forebrain neurons (Allen & Brown, 1993) and in adult mouse SCG neurons (Shapiro *et al*., 1999), but are in contrast to findings in adult rat SCG neurons (Bernheim *et al*., 1992). Since binding data indicate that both BeCh and Oxo-M have an approximately 10-fold greater affinity for M_2 *versus* M_4 receptors, it is possible that the M_4 effect is overshadowed by the M_2 effect. If so, we would predict that when M_2 receptors are blocked, high concentrations of agonist could inhibit currents using M_4 receptors. A second possibility is that in neonatal SCG, M_2 receptors mediate the membrane-delimited pathway but by adult, M_4 receptors dominate.

Separation of muscarinic-induced modulatory pathways with bethanechol

Muscarinic-induced modulation of Ca^{2+} currents by both a diffusible second-messenger signaling cascade and a membrane-delimited pathway appears not only in SCG neurons, but also in striatal medium spiny neurons, sensorimotor pyramidal cells and hippocampal CA1 neurons (Toselli *et al*., 1989; Fisher & Johnston, 1990; Toselli & Taglietti, 1995; Stewart *et al*., 1999; Hernandez-Lopez *et al*., 2000). This observation suggests that where M_1 muscarinic receptor expression has been detected (Buckley *et al*., 1988; Levey *et al*., 1991; Levey, 1993; Wei *et al*., 1994), coexpression of muscarinic-induced, membrane-delimited and diffusible second messenger modulatory pathways often occurs. Perhaps this coexpression of muscarinic receptor subtypes accounts for previous difficulties in isolating and linking

them to specific signal transduction cascades. Our demonstration that the classical muscarinic agonist BeCh selectively activates the membrane-delimited pathway, with no significant activation of the diffusible second messenger pathway, is a step towards independently manipulating these two pathways under otherwise identical conditions. Moreover, the identification of BeCh as a muscarinic agonist with apparent high selectivity for M_2 receptor stimulation of the membrane-delimited signal transduction cascade has broad implications for designing agents that target receptor subtypes. Muscarinic receptors are present in both the central and peripheral nervous systems where they play diverse roles in autonomic function, learning, memory and cognition (see Caulfield, 1993; Levey, 1993; Growdon, 1997; Perry *et al*., 1999, for reviews). Thus, more selective muscarinic agonists should help probe the role of these receptors in brain functioning and aid in the treatment of various autonomic as well as central, cognitive disorders such as Alzheimer's disease.

This study was funded by an established investigator award from the American Heart Association (ARR). We thank Claire Baldwin and John F. Heneghan for critically reading and critiquing previous versions of the paper. We thank Joshua J. Singer and John V. Walsh for helpful discussions.

References

ADEM, A. & KARLSSON, E. (1997). Muscarinic receptor subtype selective toxins. *Life Sci.,* **60,** 1069–1076.

ALLEN, T.G.J. & BROWN, D.A. (1993). M_2 muscarinic receptor-mediated inhibition of the Ca^{2+} current in rat magnocellular cholinergic basal forebrain neurones. *J. Physiol.,* **466,** 173–189.

BEAN, B.P. (1989). Neurotransmitter inhibition of neuronal calcium currents by changes in channel voltage dependence. *Nature,* **340,** 153–156.

BEECH, D.J., BERNHEIM, L. & HILLE, B. (1992). Pertussis toxin and voltage dependence distinguish multiple pathways modulating calcium channels of rat sympathetic neurons. *Neuron,* **8,** 97–106.

BEECH, D.J., BERNHEIM, L., MATHIE, A. & HILLE, B. (1991). Intracellular Ca^{2+} buffers disrupt muscarinic suppression of Ca^{2+} current and M current in rat sympathetic neurons. *Proc. Natl. Acad. Sci. USA,* **88,** 652–656.

BERNHEIM, L., BEECH, D.J. & HILLE, B. (1991). A diffusible second messenger mediates one of the pathways coupling receptors to calcium channels in rat sympathetic neurons. *Neuron,* **6,** 859–867.

BERNHEIM, L., MATHIE, A. & HILLE, B. (1992). Characterization of muscarinic receptor subtypes inhibiting Ca^{+2} current and M current in rat sympathetic neurons. *Proc. Natl. Acad. Sci. USA,* **89,** 9544–9548.

BUCKLEY, N.J., BONNER, T.I. & BRANN, M.R. (1988). Localization of a family of muscarinic receptor mRNAs in rat brain. *J. Neurosci.,* **8,** 4646–4652.

BUCKLEY, N.J., BONNER, T.I., BUCKLEY, C.M. & BRANN, M.R. (1989). Antagonist binding properties of five cloned muscarinic receptors expressed in CHO-11 cells. *Mol. Pharmacol.,* **35,** 469–476.

BYMASTER, F.P., CALLIGARO, D.O. & FALCONE, J.F. (1999). Arachidonic acid release in cell lines transfected with muscarinic receptors: a simple functional assay to determine response of agonists. *Cell. Signal.,* **11,** 405–413.

CAULFIELD, M.P. (1993). Muscarinic receptors—characterization, coupling and function. *Pharmacol Ther.,* **58,** 319–379.

CAULFIELD, M.P. & BIRDSALL, N.J.M. (1998). International Union of Pharmacology. XVII. Classification of muscarinic acetylcholine receptors. *Pharmacol. Rev.,* **50,** 279–290.

ELMSLIE, K.S., ZHOU, W. & JONES, S.W. (1990). LHRH and GTP-γ-S modify calcium current activation in bullfrog sympathetic neurons. *Neuron,* **5,** 75–80.

FERNANDEZ-FERNANDEZ, J.M., WANAVERBECQ, N., HALLEY, P., CAULFIELD, M.P. & BROWN, D.A. (1999). Selective activation of heterologously expressed G protein-gated K^+ channels by M_2 muscarinic receptors in rat sympathetic neurones. *J. Physiol.,* **515,** 631–637.

FISHER, R. & JOHNSTON, D. (1990). Differential modulation of single voltage-gated calcium channels by cholinergic and adrenergic agonists in adult hippocampal neurons. *J. Neurophysiol.,* **64,** 1291–1302.

GRABNER, M., WANG, Z., HERING, S., STRIESSNIG, J. & GLOSSMANN, H. (1996). Transfer of 1,4-dihydropyridine sensitivity from the L-type to class A (Bl) calcium channels. *Neuron,* **16,** 207–218.

GROWDON, J.H. (1997). Muscarinic agonists in Alzheimer's disease. *Life Sci.,* **60,** 993–998.

HALEY, J.E., DELMAS, P., OFFERMANNS, S., ABOGADIE, F.C., SIMON, M.I., BUCKLEY, N.J. & BROWN, D.A. (2000). Muscarinic inhibition of calcium current and M current in $G\alpha_q$-dcficicnt mice. *J. Neurosci.,* **20,** 3973–3979.

HAMILL, O.P., MARTY, A., NEHER, E., SAKMANN, B. & SIGWORTH, E.J. (1981). Improved patch-clamp techniques for high-resolution current recording from cells and cell-free membrane patches. *Pflugers Arch.,* **391,** 85–100.

HAWROT, E. & PATTERSON, P.H. (1979). Long-term culture of dissociated sympathetic neurons. *Methods Enzymol.,* **58**, 574–584.

HILLE, B. (1994). Modulation of ion-channel function by G-protein-coupled receptors. *Trends Neurosci.,* **17,** 531–536.

HERNANDEZ-LOPEZ, S., TKATCH, T., PEREZ-GARCIA, E., GALARRAGA, E., BARGAS, J., HAMM, H. & SURMEIER, D.J. (2000). D_2 dopamine receptors in striatal medium spiny neurons reduce L-type Ca^{2+} currents and excitability *via* a novel PLCβl-IP_3-calcineurin-signaling cascade. *J. Neurosci.,* **20,** 8987–8995.

IKEDA, S.R. (1991). Double-pulse calcium channel current facilitation in adult rat sympathetic neurones. *J. Physiol.,* **439,** 181–214.

IMREDY, J.P. & YUE, D.T. (1994). Mechanism of Ca(2+)-sensitive inactivation of L-type Ca2+ channels. *Neuron,* **12,** 1301–1318.

LEVEY, A.I. (1993). Immunological localization of ml–m5 muscarinic acetylcholine receptors in peripheral tissues and brain. *Life Sci.,* **52,** 441–448.

LEVEY, A.I., KITT, C.A., SIMONDS, W.F., PRICE, D.L. & BRANN, M.R. (1991). Identification and localization of muscarinic acetylcholine receptor proteins in brain with subtype-specific antibodies. *J. Neurosci.,* **11,** 3218–3226.

LIU, L., BARRETT, C.F. & RITTENHOUSE, A.R. (2001). Arachidonic acid both inhibits and enhances whole cell calcium currents in rat sympathetic neurons. *Am. J. Physiol. (Cell Physiol.),* **280,** C1293–C1305.

LIU, L. & RITTENHOUSE, A.R. (2000). Effects of arachidonic acid on unitary calcium currents in rat sympathetic neurons. *J. Physiol.,* **525,** 391–404.

LIU, L. & RITTENHOUSE, A.R. (2003). Arachidonic acid mediates muscarinic inhibition and enhancement of N-type Ca^{2+} current in sympathetic neurons. *Proc. Natl. Acad. Sci. USA,* **100,** 295–300.

MATHIE, A., BERNHEIM, L. & HILL, B. (1992). Inhibition of N- and L-type calcium channels by muscarinic receptor activation in rat sympathetic neurons. *Neuron,* **8,** 907–914.

PERRY, E., WALKER, M., GRACE, J. & PERRY, R. (1999). Acetylcholine in mind: a neurotransmittcr correlate of consciousness? *TINS,* **22,** 273–80.

PLUMMER, M.R., LOGOTHETIS, D.E. & HESS, P. (1989). Elementary properties and pharmacological sensitivities of calcium channels in mammalian peripheral neurons. *Neuron,* **2,** 1453–1463.

PLUMMER, M.R., RITTENHOUSE, A.R., KANEVSKY, M. & HESS, P. (1991). Neurotransmitter modulation of calcium channels in rat sympathetic neurons. *J. Neurosci.,* **11,** 2339–2348.

RAMPE, D. & LACERDA, A.E. (1991). A new site for the activation of cardiac calcium channels defined by the nondihydropyridine FPL 64176. *J. Pharmacol. Exp. Ther.,* **259,** 982–987.

RICHARDS, M.H. & VAN GIERSBERGEN, P.L.M. (1995). Human muscarinic receptors expressed in A9L and CHO cells:

activation by full and partial agonists. *Br. J. Pharmacol.,* **114,** 1241–1249.

RITTENHOUSE, A.R. & HESS, P. (1994). Microscopic heterogeneity in unitary N-type calcium currents in rat sympathetic neurons. *J. Physiol.,* **474,** 87–99.

SHAPIRO, M.S., GOMEZA, J., HAMILTON, S.E., HILLE, B., LOOSE, M.D., NATHANSON, N.M., ROCHE, J.P. & WESS, J. (2001). Identification of subtypes of muscarinic receptors that regulate Ca^{2+} and K^{+} channel activity in sympathetic neurons. *Life Sci.,* **68,** 2481–2487.

SHAPIRO, M.S., LOOSE, M.D., HAMILTON, S.E., NATHANSON, N.M., GOMEZA, J., WESS, J. & HILLE, B. (1999). Assignment of muscarinic receptor subtypes mediating G-protein modulation of Ca(2+) channels by using knockout mice. *Proc. Natl. Acad. Sci. USA,* **96,** 10899–10904.

STEWART, A.E., YAN, Z., SURMEIER, D.J. & FOEHRING, R.C. (1999). Muscarine modulates Ca2+ channel currents in rat sensorimotor pyramidal cells via two distinct pathways. *J. Neurophysiol.,* **81,** 72–84.

TAYLOR, P. (1980). Cholinergic agonists. In: *The Pharmacological Basis of Therapies*, 6th edn. eds. Gilman, A.G., Goodman, L.S. & Gilman, A. pp. 91–99. New York: MacMillan Publishing Co., Inc.

TOSELLI, M., LANG, J., COSTA, T. & LUX, H.D. (1989). Direct modulation of voltage-dependent calcium channels by muscarinic activation of a pertussis toxin-sensitive G-protein in hippocampal neurons. *Pflugers Arch.,* **415,** 255–261.

TOSELLI, M. & TAGLIETTI, V. (1995). Muscarine inhibits high-threshold calcium currents with two distinct modes in rat embryonic hippocampal neurons. *J. Physiol.,* **483,** 347–365.

WANKE, E., FERRONI, A., MALGAROLI, A., AMBROSINI, A., POZZAN, T. & MELDOLESI, J. (1987). Activation of a muscarinic receptor selectively inhibits a rapidly inactivated Ca^{2+} current in rat sympathetic neurons. *Proc. Natl. Acad. Sci. U.S.A.*, **84,** 4313–4317.

WANG, S.Z. & EL-FAKAHANY, E.E. (1993). Application of transfected cell lines in studies of functional receptor subtype selectivity of muscarinic agonists. *J. Pharmacol. Exp. Ther.,* **266,** 237–243.

WEI, J., WALTON, E.A., MILICI, A. & BUCCAFUSCO, J.J. (1994). ml-m5 muscarinic receptor distribution in rat CNS by RT-PCR and HPLC. *J. Neurochem.,* **63,** 815–821.

(Received July 26, 2002
Revised October 11, 2002
Accepted October 23, 2002)